Applied Energy 206 (2017) 70–82

Contents lists available at ScienceDirect

Applied Energy

journal homepage: www.elsevier.com/locate/apenergy

Experimental and numerical performance analysis of a TC-Trombe wall

Bendong Yu[a], Wei He[b,*], Niansi Li[a], Liping Wang[b], Jingyong Cai[a], Hongbing Chen[c], Jie Ji[a], Gang Xu[d]

[a] Department of Thermal Science and Energy Engineering, University of Science and Technology of China, Hefei 230026, China
[b] Department of Building Environment and Equipment, Hefei University of Technology, Hefei 230009, China
[c] School of Environment and Energy Engineering, Beijing University of Civil Engineering and Architecture, Beijing 100044, China
[d] Key Laboratory for Renewable Energy and Gas Hydrates, Guangzhou Institute of Energy Conversion, Chinese Academy of Sciences, No. 2 Nengyuan Road, Tianhe District, Guangzhou 510640, China

HIGHLIGHTS

- A novel zero-energy TC-Trombe wall was introduced.
- Experimental testing platform and numerical model were built.
- The air heating and HCHO degradation performance were analyzed experimentally.
- A photothermocatalytic synergetic effect existed in the solar driven TCO.
- The total saving energy of 97.4 kW h/m^2 be obtained in heating seasons in Hefei.

ARTICLE INFO

Keywords:
Trombe wall
Thermal catalytic
Thermal properties
Space heating
Solar energy
Photothermocatalytic synergetic effect

ABSTRACT

The present paper proposes a novel zero-energy solar application system combining the thermal catalytic technology with Trombe wall (TC-Trombe wall), which could realize indoor air purification and space heating simultaneously fully driven by solar energy. A full-day experiment was conducted to study the air heating performance and formaldehyde degradation performance of TC-Trombe wall. Results showed that the daily air heating efficiency was 41.3%. In our experiments, the generated total volume of fresh air and total formaldehyde degradation amount by TC-Trombe wall were 249.2 m^3/(m^2 day) and 208.4 mg/(m^2 day), respectively. In addition, a photothermocatalytic synergetic effect exists in the solar light driven thermocatalytic oxidation process over MnO_x-CeO_2 catalysts. A dynamic numerical model was developed to predict system thermal properties. Based on the simulation results, the effects of the solar radiation intensity, ambient temperature and air layer thickness on the system thermal efficiency were discussed. Furthermore, the energy saving performance of TC-Trombe wall was evaluated in heating seasons in Hefei based the established system thermal model. Results showed that the total saving energy of up to 97.4 kW h/m^2 could be obtained. The saving energy for space heating and formaldehyde degradation were 64.3 kW h/m^2 and 33.1 kW h/m^2, respectively.

1. Introduction

Parallel to the high speed development of economy and rapid growth of human population, the environmental pollution and lack of energy are two main problems in the new century. The building energy consumption for the heating, ventilating and air conditioning (HVAC) occupies 30–40% of the total energy consumption in the world to maintain a comfortable and health indoor environment [1]. The ratio of building energy consumption for space heating should not be ignored. Therefore, it is potential to use the renewable energy such as solar energy for building space heating.

Trombe wall (TW) has been popularized as one kind of solar space heating methods in the past few decades because it delivers some advantages such as simple configuration, low running cost and using the storing solar energy of the wall during daytime to heat room overnight [2–4]. Typical Trombe wall consists of a glass plate, massive wall, air channel and vents [5]. The high thermal mass wall can store solar heat in the day and release it into the room in the night. And the energy stored performance of wall is a very important parameter to a Trombe wall system for night heating. Hassanain et al. [6] found that the

* Corresponding author.
E-mail address: Hwei@hfut.edu.cn (W. He).

http://dx.doi.org/10.1016/j.apenergy.2017.08.171
Received 13 April 2017; Received in revised form 15 August 2017; Accepted 16 August 2017

Nomenclature

G	solar radiation intensity, W/m^2
H	height, m
A	area, m^2
c	specific heat capacity, J/(kg K)
T	temperature, °C
d	hydrodynamic diameter, m
Pr	Prandtl number
Ra	Rayleigh number
Nu	Nusslet number
Re	Reynolds number
E	electricity
Ra	rayleigh number
m	mass, kg; mass flow, kg/s
Q	volumetric flow rate of gas, m^3/h
f	resistance factor
h	heat transfer coefficient, W/(m^2 K)
C	formaldehyde concentration, ppb
R	thermal resistance
F	view factor
t	time, s
V	air flow velocity, m/s; volume, m^3

Greeks

ρ	density of catalyst, kg/m^3
δ	thickness, m
λ	thermal conductivity, W/(m K)
ε	formaldehyde once-through conversion
α	absorptivity
σ	Stefan-Boltzmann constant, W/(m^2 K^4)
τ	transmissivity
η	efficiency
β	coefficient of thermal expansion, K^{-1}
ν	dynamic viscosity of air, m^2/s

Subscripts

th	thermal
a	air
HCHO	formaldehyde
cata	catalyst
eq	equivalent
in	inlet
out	outlet
ti	heat insulating material
conv	convective heat transfer
rad	radiation heat transfer
g	glass plate

Abbreviation

TCO	thermal catalytic oxidation
TW	Trombe wall
VOCs	volatile organic compounds
PCO	photocatalytic oxidation
RSMD	root mean square deviation
CADR	clean air delivery rate, m^3/h
IAQ	Indoor Air Quality
ppb	parts per billion
HVAC	heating, ventilating and air conditioning

average indoor air and soil temperature increased 1.1 °C and 4 °C during winter nighttime in the greenhouse when Trombe wall was used for the solar heat storage. Hernandez et al. [7] found that storage wall could supply the maximum energy stored of about 109 MJ and 70 MJ to the room in nighttime during the warmest day and the warmest day in Mexico, respectively. Liu et al. [8] investigated the heat storage and release of Trombe wall in the fully day based on the numerical analysis. Results showed that the massive wall released heat from 15:00 PM to 7:30 AM and stored heat from 7:30 AM to 15:00 PM. A balance between heat storage and heat release was achieved at about 7:30 AM. Rabani et al. [9] compared the energy storage rate and time duration of room heating during the non-sunny periods using four different materials of the Trombe wall such as concrete wall, brick wall, hydrated salt wall and paraffin wax. Results showed that the Trombe wall made of paraffin wax could keep the room more warm in comparison with other materials for about 9 h. The influencing factors such as the thickness of the core layer [10], the massive wall thickness and the existence of a ventilation system [11], integrating phase change materials [12], and the shading effect of the side walls [13], on the heat release performance were investigated in night time in Trombe wall system.

However, it exists several inevitable shortcomings such as the low thermal resistance [14], single-function [3], and some aesthetical problems because the wall is colored black to increase the absorptivity of wall [15] in Trombe wall system. Furthermore, the paint layer might release the volatile organic compounds (VOCs) when it reached high temperature under solar radiation. Therefore, many improved Trombe wall systems have been developed [15–18].

The adding of another insulation layer or closed air layer leads to the increase of the thermal resistance of the composite TW [16,19]. The amplitudes of the indoor temperature for the composite TW are smaller than that of the classical TW. Tunc et al. [18] filled the air cavity with the high-absorptivity and low-density particles in TW. Results showed that the heat collecting efficiency got the great improvement because the air in air cavity was in contact with the fluidized particles directly.

The modifications to TW such as Trans-wall and photovoltaic TW make itself be more multifunctional. More high value-added products such as electricity, thermal comfort and aesthetic enjoyment are produced. Trans-wall provides not only heat but also illumination of the room [17]. Another novel design is photovoltaic TW (PV-TW) that simultaneously realizes both space heating and electricity generation [15,20,21]. The generated electricity is the high value-added product compared with thermal energy. In general, the air flow behind the PV panels has a cooling effect on the PV cells, which is beneficial to the electrical performance of PV cells [22]. Moreover, PV-TW solves aesthetic problem of traditional TW perfectly because the deep blue color of PV cells makes the external facade more appealing [15]. Ji et al. [15,23–25] proposed PV-TW and conducted a series of investigations including experiments and models on the performance of space heating and electricity generation. Various factors such as south facade designs [15], PV coverage ratio [23], areas and climatic conditions [26–28], and ventilation modes including natural ventilation and mechanical ventilation [29], affecting thermal and electrical efficiency were discussed in detail. However, compared with the conventional TW, the thermal efficiency of PV-TW reduces due to the opaque nature of PV cells. Sun et al. [15] pointed out the thermal efficiencies of PV Trombe wall reduced by 7% and 17% for the different fractions of PV coverage of 33.4% and 100%, respectively. And the replacement of PV cells by semi-transparent amorphous silicon solar cell would decrease the daily average electrical efficiency of the system greatly [30]. Another novel designs including PV blinds-Trombe wall [31] and PV thermoelectric-Trombe wall [32] were studied to improve the functionality, thermal and electrical efficiency.

As mentioned, nowadays, human beings have put more and more focus on the Indoor Air Quality (IAQ) of dwelling buildings and public

buildings due the accumulation of pollutants caused by tight rooms [33–34]. In the current air-conditioning system, the outdoor air ventilation is an effective method to dilute and remove indoor air pollutants [35,36]. Ben-David et al. [37] used the carbon dioxide and formaldehyde as model pollutants to compare the influences of natural ventilation and mechanical ventilation on the IAQ. As we know the energy saving potential is strongly influenced by the outdoor air quality whether under natural ventilation or mechanical ventilation [36,38,39]. However, an indisputable fact is that the outdoor pollution problem has been gotten worse and worse due to the large-scale use of fossil fuel, automobile exhaust, and factories discharge especially in the most densely populated areas of the world [38]. However, the outdoor air intake would be decreased if the indoor pollutant were degraded locally. Cui et al. [40] proposed a hybrid system combining air purification system and cooling system. This system uses ozone-based oxidation treatment technology to purify the return air. They aim to decrease the outdoor air intake when improving IAQ through ventilation. Results showed that an annual energy consumption saving of up to 64.6 kW h/m^2 could be obtained by analyzing the combined system. However, the adding of ozone-based purification unit including ozone generator, reactor and ozone destruction unit increases the complexity of the system and maintenance cost. Moreover, the excess ozone is harmful to human health.

At the same time, persistent advanced studies have been carried out to develop highly efficient and low-cost technologies for the degradation of indoor VOCs [41,42]. Solar photocatalytic technology (PCO) has been gotten great attention because it is one of the most promising technologies to use solar energy for degradation of pollutants. However, the ultraviolet light, which is the mainly efficient part to PCO technology, only occupies about 5% in the range of solar spectrum. And the ratios of visible light and infrared light parts are 45% and 50%, respectively. Therefore, the utilization of PCO to solar energy is very limited. Thermal catalytic oxidation (TCO) is an efficient and promising technique to pollutants removal driven by thermal energy [43–47]. The driven force of TCO technology is the thermal energy that can be derived from full solar spectrum light especially including visible and infrared light parts. Therefore, it is potential to develop full solar spectrum light driven TCO to degrade indoor VOCs. An interesting idea is the combination of TW and TCO technology (TC-Trombe wall), which can perfectly use absorbed thermal energy to obtain the high value-added clean air at the same time of heating indoor air. As we known, for conventional Trombe wall, the thermal energy of heat absorption surface is only used for heating the air. But for TC-Trombe wall, this thermal energy for driving the TCO reaction is still used for space heating finally. The thermal performance has no reduction compared with the conventional TW. The combination of Trombe wall with solar TCO technology is firstly introduced here, which is significant for the broadening the application of Trombe wall.

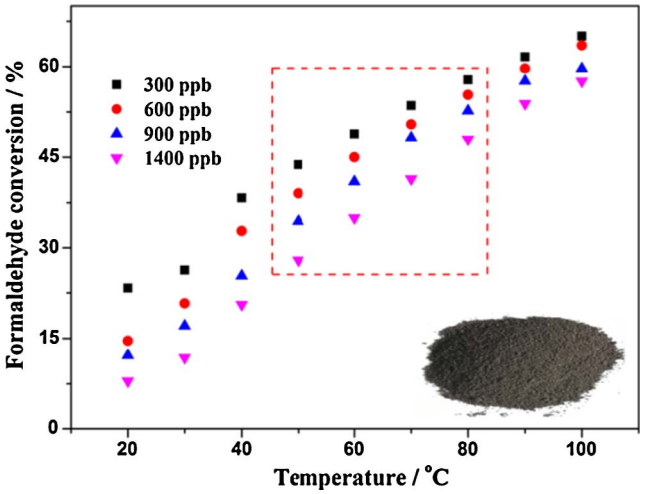

Fig. 2. Temperature dependence of formaldehyde conversion over MnO_x-CeO_2 under different formaldehyde concentrations [43].

The article aims to (1) propose the novel zero-energy TC-Trombe wall and build experimental testing platform of TC-Trombe wall, (2) investigate the system solar collecting performance and formaldehyde degradation performance, (3) build the system thermal model to predict the system performance, and (4) investigate the saving energy consumption of TC-Trombe wall in heating seasons in Hefei.

2. System descriptions

As shown in Fig. 1, the thermal catalytic materials are coated on the surface of external wall. The catalysts layer is heated under solar radiation and approaches certain temperature. Then indoor air with contaminants enters into the air cavity with the effect of buoyancy lift. The contaminants are degraded by the heated catalysts layer when the catalysts layer approaches the start-off temperature of a TCO reaction. The clean air enters into the room. At the same time, the space heating mode is realized.

We have talked about the feasibility analysis of solar driven TCO degradation indoor gaseous formaldehyde over MnO_x-CeO_2 [43]. Fig. 2 shows the formaldehyde conversion under different initial concentration and temperature levels over MnO_x-CeO_2 catalysts. Under typical indoor concentration levels of several times than legal limiting concentration (80 ppb) [48], the formaldehyde single-pass conversion

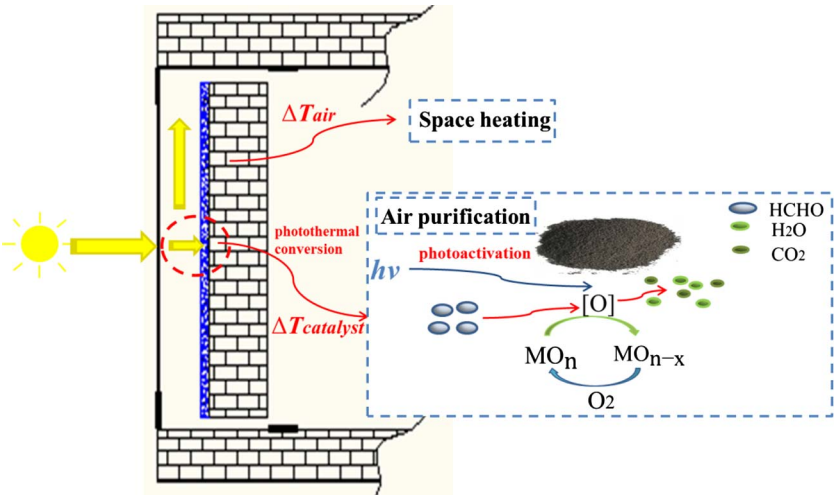

Fig. 1. A novel concept of the combination of Trombe wall and indoor air purification technology for space heating and formaldehyde degradation.

could approach 30–60% at the temperature of 40–80 °C. In current research on TW, this temperature levels can be obtained easily [2,3].

3. Experimental

3.1. Description of the experimental set-up

To investigate the thermal and formaldehyde degradation performance of TC-Trombe wall in the real environment, we built an experimental testing system. Fig. 3 shows the schematic diagram of experimental set-up of TC-Trombe wall. Compared with traditional TW, there is the catalyst layer between the air cavity and insulation layer, which realizes two functions i.e. solar-thermal conversion and thermal catalytic oxidation. From outside to inside, in turn, are glass cover, air cavity, catalysts layer, thermal insulation material layer, and air inlet and outlet. The main structure sizes of TC-Trombe wall are shown in Table 1.

The preparation of catalysts MnO_x-CeO_2 has been described previously [43]. Firstly, the prepared catalyst powders were grounded into the uniform particle size (about 100–200 mesh). Secondly, the uniform powders were dispersed into a certain amount of deionized water. A uniform black suspension solution was formed after stirring for 30 min. Thirdly, the obtained uniform black suspension solution was coated on the thin aluminum plate and dried the coated thin catalytic layer for 20 min under 80 °C in the drying oven. The coating and drying processes were conducted circulated for several times. The obtained the catalyst layer was dried for 8 h under 100 °C to remove all water. Then the desired catalysts layer was obtained. The mass of catalyst in our experiments was 5 g. To investigate the solar-thermal conversion performance of our prepared catalyst, the diffusive reflectance UV–Vis-IR absorption spectra were recorded on a UV-3600 spectrophotometer from Instruments' Center for Physical Science, University of Science and Technology of China.

3.2. Test procedure and instruments

The experimental testing system was mounted in University of Science and Technology of China, Hefei (32°N, 117°E), which was applied as the south facade. A list of experimental testing and monitoring apparatus was given in Table 2. The testing parameters included temperature, wind speed, vertical global solar radiation intensity and formaldehyde concentration. The temperature testing included the glass cover temperature, air temperature in the air cavity, catalysts layer temperature, air inlet and outlet temperature and ambient temperature. Copper-constantan thermocouple thermometers were used to measure the experimental temperature. The temperature testing points were marked in Fig. 3. The temperature data were recorded with an interval of 30 s. Hot-wire anemometer measured the air velocity in the cavity every 10 min. The testing sections of formaldehyde degradation performance in TC-Trombe wall included gas generating section and gas detection section. The formaldehyde standard gas (30 ppm) purchased from Hefei Long-xing Electric Appliance Ltd used as the pollutant source. As shown in Fig. 3, a certain concentration of gaseous formaldehyde was obtained by blowing constant amount formaldehyde standard gas into the air inlet. Formaldehyde detector MS-400 purchased from Anqing Chang-jia Electronics Ltd. measured the inlet and outlet formaldehyde concentration every 10 min. The experimental initial formaldehyde concentration range was 400–900 ppb. Table 2 shows the accuracy of experimental measuring apparatus. The experiments were conducted from 8:30AM to 16:30 PM in 12th February 2017.

4. Data analysis and system model

4.1. Performance evaluation

The performance of TC-Trombe wall can be characterized by the thermal efficiency and formaldehyde removal efficiency. The thermal efficiency is evaluated by the obtained thermal energy of the air in air cavity form the total received solar radiation. The instantaneous thermal efficiency can be defined as following:

$$\eta_{th} = \frac{m_a c_a (T_{out} - T_{in})}{A G_{solar}} \tag{1}$$

where m_a, kg/s, and c_a, J/(kg K), are the air mass flow in the air cavity and specific heat of air, respectively. T_{out} and T_{in} are air inlet temperature and air outlet temperature, respectively. A, m^2, is the received area of solar energy, and G_{solar}, W/m^2, is the solar radiation intensity. And the daily thermal efficiency can be obtained from the time integral of equation (1).

$$\overline{\eta_{th}} = \frac{\int m_a c_a (T_{out} - T_{in}) dt}{\int A G_{solar} dt} \tag{2}$$

We can evaluate the air purification properties of TC-Trombe wall by several common indexes such as once-through conversion, clean air delivery (CADR), air purification rate referring to the evaluation methods of air cleaners [49,50]. These evaluation indexes can characterize the pollutant-removal efficiency and energy cost of an air cleaner to some extent.

Formaldehyde once-through conversion can be calculated according to the following equation:

$$\varepsilon = \frac{C_{in} - C_{out}}{C_{in}} \tag{3}$$

where C_{in} and C_{out}, ppb, are the inlet and outlet formaldehyde concentration, respectively.

The clean air delivery (CADR) is defined as the volume of fresh air generated per hour. It is can be expressed as the product of the air volume flow (m^3/h) and once-through conversion. And the daily clean air amount can be obtained from the time integral of CADR.

$$CADR = Q\varepsilon \tag{4}$$

$$V_{total} = \int_0^\tau CADR dt \tag{5}$$

The amount of clean air delivery per unit of energy input, CADR/P, can be used as the assessment criteria of energy consumption and economic level for an air cleaner [45]. And P is the input energy including fan and electrical heater.

Air purification rate, mg/s, is defined as the degradation mass of formaldehyde per second, can be expressed as following:

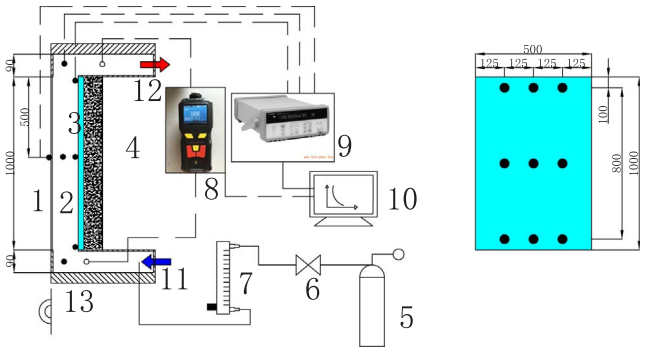

Fig. 3. Schematic diagram of the experimental set-up of TC-Trombe wall. (1) Glazing. (2) Air cavity. (3) Catalyst layer. (4) Thermal insulation material layer. (5) Formaldehyde standard gas. (6) Valve. (7) Flowmeter. (8) Formaldehyde detector. (9) Data acquisition instrument. (10) Computer. (11) Air inlet. (12) Air outlet. (13) Solar pyranometer.

Table 1
The detailed structure sizes of TC-Trombe wall.

	Symbol	Unit	Value
Bottom vent area	A_{in}	m^2	0.028
Top vent area	A_{out}	m^2	0.028
Solar received area	A	m^2	0.5
Height	H	m	1
Air cavity thickness	δ_a	m	0.09
Air cavity width	D	m	0.5
Glass cover thickness	δ_g	m	0.005
Insulation layer thickness	δ_{ti}	m	0.3
Catalysts layer thickness	δ_{cata}	μm	7

Table 2
The accuracy of experimental measuring apparatus.

Apparatus	Accuracy
Formaldehyde detector MS-400	2%
Hot-wire anemometer KANOMAX	± 0.01 m/s
Copper-constantan thermocouple thermometer	± 0.5 °C
Solar pyranometer TBQ-2	± 11.04 μv/(W m^2)
Data acquisition 34970A	–
Air flow meter LZB-3W	± 2.4 ml/min

$$m_{HCHO} = Q(C_{in}-C_{out}) \tag{6}$$

Substituting the Eq. (3) back into Eq. (6), the expression of air purification rate is obtained as follows:

$$m_{HCHO} = Q\varepsilon C_{in} \tag{7}$$

And the daily degradation mass of formaldehyde can be obtained from the time integral of Eq. (7), which is expressed as following:

$$m_{total} = \int_0^{\tau} m_{HCHO}\,dt \tag{8}$$

For the two essentially different efficiencies i.e. thermal efficiency and formaldehyde removal efficiency, it is hard to evaluate the integrated performance of TC-Trombe wall. However, as we known, the absorbed solar energy by the catalysts layer is used for heating the catalysts layer. Then the catalysts layer heats the air in the air cavity. And the thermal catalytic oxidation reaction is motivated when the catalysts layer reaches the start-off temperature after absorbing enough heat energy under solar radiation. Therefore, formaldehyde removal efficiency can be reflected in the thermal storage performance of the catalysts layer. Therefore, we can define the formaldehyde degradation efficiency in TC-Trombe wall as follows:

$$\eta_{\mathrm{HCHO}} = \frac{E_{\mathrm{HCHO}}}{AG_{solar}} \tag{9}$$

where E_{HCHO} was the electricity cost if the adsorbed heat energy by the catalysts layer used for formaldehyde degradation section came from the electrical heater not the solar energy.

Therefore, the integrated efficiency of TC-Trombe wall considering the thermal efficiency and formaldehyde removal efficiency can be expressed as follows:

$$\eta_{total} = \eta_{th} + \eta_{\mathrm{HCHO}} \tag{10}$$

4.2. System thermal model

To analyze the system thermal collecting performance, this section established system dynamic thermal model. The formaldehyde reaction heat is ignored because the indoor formaldehyde concentration is very low [43–45]. The model includes three components of the glass cover, air cavity and catalysts layer. In this model, the material thermal properties such as specific heat capacity and thermal conductivity are considered as the constants.

The heat transfer in the glass cover is considered as a one-dimensional heat conduction model because the heat transfer in the thickness direction can be ignored. And heat balance expression in the glass cover is as follows:

$$\rho_g\delta_g c_g\frac{\partial T_g}{\partial t} = \lambda_g\delta_g\frac{\partial^2 T_g}{\partial y^2} + h_{conv-rad}(T_{eq}-T_g) + h_{conv,a,g}(T_a-T_g) + h_{rad,cata,g}(T_{cata}-T_g) + G\alpha_g \tag{11}$$

where T_g is the temperature of the glazing, °C, t is the time, s, λ_g is the thermal conductivity, W/(m K), ρ_g is the density, kg/m^3, y is the height direction, m, δ_g is the thickness of the glazing, m, α_g is the absorptivity. The second to last item in the right side of the equation are the heat transfer between the glass cover and ambient environment, heat convection between the glass cover and air in the cavity air, radiation heat transfer between the glass cover and catalysts layer, and the absorbed solar flux by the glass cover, respectively. T_{eq} is the equivalent temperature, which is considered to be equal to the outdoor air temperature, and $h_{conv\text{-}rad}$ has a standard value of 29 W/(m^2 K) [43].

The air in the channel of TC-Trombe wall has convective heat exchange with the catalysis layer and glass cover. And the energy balance of air in the air cavity in vertical direction is as follows:

$$\rho_a\delta_a c_a\frac{\partial T_a}{\partial t} = h_{conv,g,a}(T_g-T_a) + h_{conv,cata,a}(T_{cata}-T_a) - \rho_a V_a\delta_a c_a\frac{\partial T_a}{\partial y} \tag{12}$$

where $h_{conv,g,a}$ and $h_{conv,cata,a}$ are the air cavity convective heat transfer coefficients with the glass cover and catalysts layer, respectively. V_a is the air bulk velocity under natural convection conditions and the expression is talked in the next section.

The catalysts layer has convective heat exchange with the air cavity, radiation heat exchange with the glass cover, absorbed solar radiation filtered by glass cover and heat loss.

$$\rho_{cata}\delta_{cata}c_{cata}\frac{\partial T_{cata}}{\partial t} = \lambda_{cata}\delta_{cata}\frac{\partial^2 T_{cata}}{\partial y^2} + h_{conv,cata,a}(T_a-T_{cata}) + h_{rad,cata,g}(T_g-T_{cata}) + \frac{(T_{eq}-T_{cata})}{R} + G\tau_g\alpha_{cata} \tag{13}$$

$$R = \frac{\delta_{ti}}{\lambda_{ti}} + \frac{1}{h_{conv-rad}} \tag{14}$$

where R is the thermal resistance between the catalysts layer and the ambient. δ_{ti} and λ_{ti} are the thickness and thermal conductivity of the heat insulating material, respectively. τ_g is the transmissivity of the glass cover. α_{cata} is the absorptivity of the catalysts layer and is calculated from the UV–vis-IR absorption spectra in Section 4.1. And δ_{cata} is the thickness of the catalysis layer and can be calculated from the following expression:

$$\delta_{cata} = \frac{m_{cata}}{\rho_{cata}A_{cata}} \tag{15}$$

where m_{cata} and ρ_{cata} are the mass and density of the coated catalysts on the thin aluminum plate, respectively. A_{cata} is the sectional surface area of the catalysts layer in the height direction.

The convective heat transfer coefficient in the air cavity can be calculated by the natural convection empirical equation of vertical plate equation for laminar or turbulent flow [51]:

$$Nu = 0.68 + \frac{0.670Ra^{1/4}}{[1+(0.492/Pr)^{9/16}]^{4/9}} \quad Ra < 10^9 \tag{16}$$

$$Nu = \left(0.825 + \frac{0.387Ra^{1/4}}{[1+(0.492/Pr)^{9/16}]^{8/27}}\right)^2 \quad Ra > 10^9 \tag{17}$$

$$Ra = \frac{g\beta(T_g-T_a)H^3}{\nu\alpha} \tag{18}$$

$$h_{conv} = \frac{Nu\lambda_a}{H} \tag{19}$$

where the characteristic length in characteristic number is the height of air cavity, H, m. The calculation method of radiation heat transfer coefficient was described in our previous study [43]. The detail computational parameters used in the model was shown in Table 3.

Root mean square deviation (RSMD) is used to analyze the error between the model values and experiment values and is expressed as follows:

$$RSMD = \sqrt{\frac{\sum [(X_{sim,i} - X_{exp,i})/X_{exp,i}]^2}{n}} \tag{20}$$

5. Results and discussion

5.1. System performance analysis

The light absorbing property of the MnO_x-CeO_2 catalysts layer plays an important role for the integrated efficiency of TC-Trombe wall. Good optical absorption property in the full solar spectrum greatly improves the space heating efficiency and formaldehyde degradation capacity. Fig. 4 shows the UV–vis-IR absorption spectra of MnO_x-CeO_2. Apparently, as shown in Fig. 4, MnO_x-CeO_2 exhibits strong absorption in whole region of solar spectrum from 200 nm to 1600 nm and the values of spectrum absorptivity are in the range of 0.92–0.98. The value of absorptivity of MnO_x-CeO_2 is close to the black paint layer or absorber plate (about 0.95 [52]) and is larger than common massive wall (about 0.7 [53]), which indicated the thermal performance of TC-Trombe wall has no reduction compared with the conventional TW. For comparison, we measured the UV–vis-IR absorption spectra of TiO_2 (P25), a common used benchmark photocatalyst. Results showed that P25 only behaved the strong absorption in the UV region and almost had no response to other spectra region. Therefore, MnO_x-CeO_2 catalysts has excellent light absorbing property, which has the huge potential of realizing highly heat collecting efficiency and considerable increase of catalysts layer temperature. The mean absorptivity of MnO_x-CeO_2 could be calculated from the following expression [51]:

$$\alpha_{cata} = \frac{\int_{\lambda_1}^{\lambda_2} \alpha(\lambda) I(\lambda) d\lambda}{\int_{\lambda_1}^{\lambda_2} I(\lambda) d\lambda} \tag{21}$$

A full-day test of TC-Trombe wall for space heating and formaldehyde degradation was conducted. Fig. 5 shows the variations of inlet and outlet air temperature of the system. The air mass flow was in the range of 0.01–0.016 kg/s according to the measurement results of the hot-wire anemometer. The air outlet temperature and air temperature variation between the inlet and outlet basically presented the similar trend as the solar radiation intensity. Air outlet temperature could approach to the maximum temperature of 37 °C at 13:24 PM. While the maximum temperature variation between inlet and outlet air temperature was 16 °C at 13:13 PM. As we known, the temperature increase was related to the solar radiation intensity and inlet air temperature. Although the maximum solar radiation was obtained at 12:58, the inlet and ambient temperature usually ascended until 14:00 PM.

Fig. 6 shows the instantaneous thermal efficiencies for space heating in TC-Trombe wall applying the Eq. (1). The instantaneous thermal efficiencies were basically located in the range of 0.2–0.6. The thermal efficiency was related to the solar radiation intensity and inlet air temperature. We fitted the instantaneous thermal efficiencies points by the method of parabola fitting, which was expressed as black imaginary line in Fig. 6. According to the fitting results, the instantaneous thermal efficiency approached the maximum of 0.512 at 10:50 AM. The daily thermal efficiency was 0.413 calculated from the Eq. (2).

In general, the thermal catalytic conversion of formaldehyde increases with the catalyst temperature [43–45]. The temperature of catalysts layer is a key factor to the system air purification efficiency. From Fig. 4, the prepared catalysts MnO_x-CeO_2 had strong absorption in whole region of solar spectrum. Fig. 7 shows the full-day catalysts layer temperature curve versus time. The catalysts temperature reached 60–90 °C after 9:30 AM, which indicated that our prepared catalysts had excellent photothermal conversion efficiency under real solar radiation. From Fig. 2, our catalysts could get the good catalytic activity under the obtained temperature range of 60–90 °C. Fig. 8 shows the formaldehyde initial concentration, outlet concentration and formaldehyde once-through conversion curves versus time. Initial formaldehyde concentration was constantly changing with the time because the air mass flow in the air cavity was changing every moment under natural convection conditions. As shown in Fig. 8, the initial formaldehyde concentration range in our experimental conditions was 400–800 ppb. The initial formaldehyde concentration values were in the range of typical indoor concentration levels [54,55].

As shown in Fig. 8, the formaldehyde single-pass conversion ε approached 30–60% under the experimental formaldehyde concentration levels. From our previous research, the formaldehyde single-pass conversion increased with the catalyst temperature rise, while decreased with the increase of concentration under typical indoor formaldehyde concentration levels [43]. The high photothermal conversion ability of catalysts layer resulted in a considerable increase of temperature. The TCO reaction started when the temperature reached to the start-off temperature over the MnOx-CeO_2 catalysts. The formaldehyde single-pass conversion curve also presented the parabola-type trend. At the beginning, on the one hand, the increase of air mass flow caused by the rise of temperature variation between inlet air temperature and outlet temperature in the cavity resulted in the decrease of initial formaldehyde concentration. On the other hand, the catalysts layer temperature increased with the rise of solar radiation intensity. The two aspects leaded to the ascending of the formaldehyde single-pass conversion. Then ε approached the maximum at noon. At last it gradually dropped after noon because of the decrease of catalysts layer temperature and the increase of formaldehyde concentration caused by the decrease of air mass flow in the air cavity. Anyhow, the formaldehyde single-pass conversion value of 30–60% has promising applications in solar driven indoor air purification. Although it is hard to make the

Table 3
Detail computational parameters for the TC-Trombe wall model.

	Symbol	Explanation	Unit	Value
Glazing	ρ_g	density	kg/m^3	2500
	c_g	specific heat capacity	J/(kg K)	840
	α_g	absorptivity	–	0.1
	τ_g	transmissivity	–	0.9
	ε_g	emissivity	–	0.9
Catalyst	ρ_{cata}	density	kg/m^3	1287
	c_{cata}	specific heat capacity	J/(kg K)	900
	λ_{cata}	thermal conductivity	W/(m K)	112
	α_{ab}	absorptivity	–	0.94
	ε_{ab}	emissivity	–	0.94
Air	ρ_a	density	kg/m^3	1.18
	c_a	specific heat capacity	J/(kg K)	1100
	λ_a	thermal conductivity	W/(m K)	0.026
	ν_a	kinematic viscosity	m^2/s	$1.58 * 10^{-5}$
Heat insulating material	ρ_a	density	kg/m^3	150
	c_a	specific heat capacity	J/(kg K)	233
	λ_a	thermal conductivity	W/(m K)	0.035
HCHO standard gas	C	concentration	ppm	30
	P	pressure	MPa	9.0
	V	volume	L	8

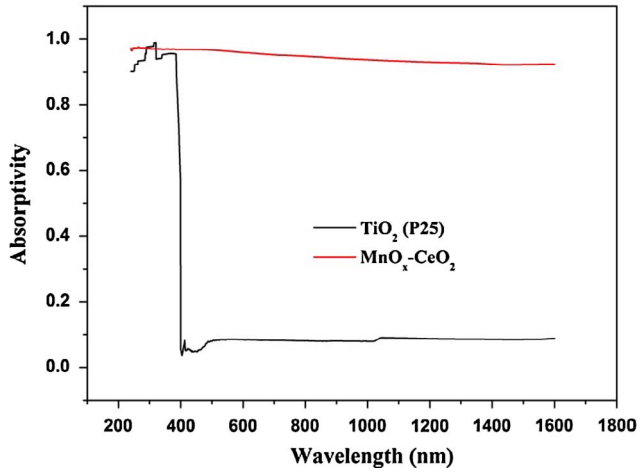

Fig. 4. UV–vis-IR absorption spectra of MnO_x-CeO_2.

formaldehyde concentration be below the WHO guideline concentration for indoor formaldehyde (80 ppb) through the single-pass conversion [48]. The indoor formaldehyde concentration will approach to or be below the standard value through long time degradation circularly.

Fig. 9 shows the clean air delivery rate (CADR) curve versus time in TC-Trombe wall. The value of CADR was in the range of 8–24 m^3/h under our experimental conditions. The total volume of fresh air generated by TC-Trombe wall was 124.6 m^3 calculated by Eq. (5). The purification rate curve versus time was also shown in Fig. 9. The total formaldehyde degradation amount by TC-Trombe wall was 104.2 mg calculated by Eq. (8). For per unit of solar receiving area, the total volume of fresh air and total formaldehyde degradation amount were 249.2 m^3/(m^2 day) and 208.4 mg/(m^2 day), respectively. Although the values might be small compared with other active systems [45,56]. However, the value of CADR is related to the mass of catalyst, system structure sizes and so on except for the essential catalytic properties of catalyst. Furthermore, TC-Trombe wall is a zero-energy consumption system driven by solar energy. The amount clean air delivery of per unit of energy input, CADR/*P*, could be infinite in theory.

Fig. 10 shows the thermal efficiency, formaldehyde removal efficiency and system integrated efficiency curves versus time applying the Eqs. (1), (9) and (10). From the curves, the formaldehyde removal efficiencies were in the range of 0.1–0.2. The invaluable clean air could be obtained in TC-Trombe wall although the values of formaldehyde removal efficiencies were small compared with that of thermal efficiencies. As we known, for conventional Trombe wall, the absorbed thermal energy by heat absorption surface is only used for heating the air. TC-Trombe wall can use this part of thermal energy to obtain clean air at the same time of heating indoor air. In reality, this part thermal energy is still used for heating air finally. The daily thermal efficiency, formaldehyde removal efficiency and system integrated efficiency were 41.3%, 12.8% and 54.1%, respectively.

5.2. Photothermocatalytic synergetic effect

To investigate why the TC-Trombe wall exhibited the excellent formaldehyde catalytic oxidation performance under solar radiation, we conducted the formaldehyde single-pass conversion experiments over MnO_x-CeO_2 under different temperature obtained by Xe lamp or electrical heater. The formaldehyde single-through experimental apparatus was referred to our previous study [57]. The light resource was a Xe lamp (CHF-XM500), which had a spectrum similar to that of solar light [58]. In the dark condition, the heat resource was the silicon heating sheet. 0.2 g catalyst samples were coated on aluminum plate. Under light radiation, the aluminum plate was adhered to thermal insulation slice to reduce the energy loss. Then put at the bottom of the reactor. In the dark experiments, the aluminum plate was adhered to the bottom of the stainless steel reactor. The reactor bottom was in contacted with the silicon heating sheet directly. Different reaction temperatures were obtained by controlling the distance between the reactor and Xe light under the condition of light radiation and the power of silicon heating sheet under the condition of in the dark, respectively. The air flow was 600 ml/min and the formaldehyde initial concentration was 600 ppb. From Fig. 11, at the same catalysts temperature, the formaldehyde single-pass conversion under solar radiation was higher than that of in the dark. At the temperatures of 40, 60, 80 and 100 °C, the formaldehyde single-pass conversion under solar radiation were 1.3, 1.2, 1.2 and 1.1 times higher than that of in the dark, respectively. It seems that a photothermocatalytic synergetic effect exists in TCO process of TC-Trombe wall.

The catalytic mechanism of MnO_x-CeO_2 catalysts under solar radiation may behave in two aspects: (1) photocatalytic oxidation mechanism [42,59,60]; (2) solar light driven thermocatalytic oxidation mechanism and photothermal conversion mechanism in full solar spectrum [58,61–63]. To confirm whether the PCO mechanism was dominant in TC-Trombe wall, we compared the formaldehyde single-

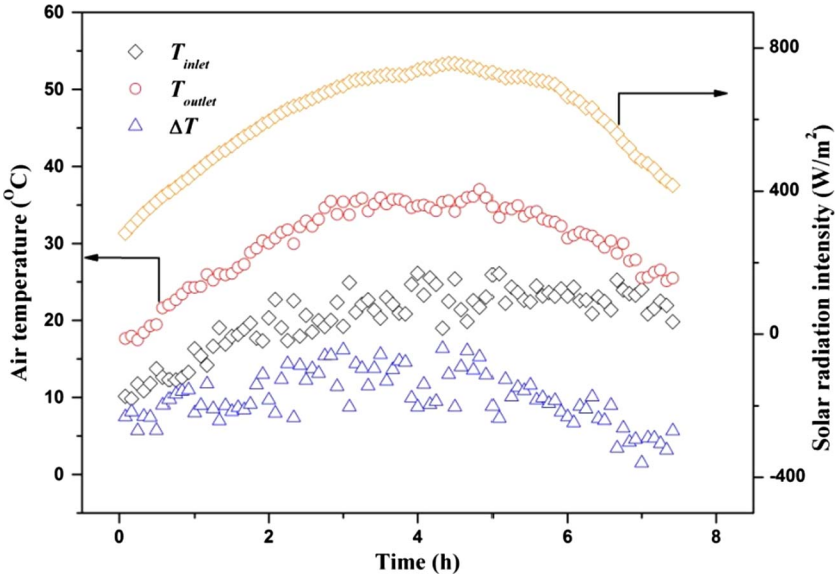

Fig. 5. Variation of inlet and outlet air temperature in TC-Trombe wall.

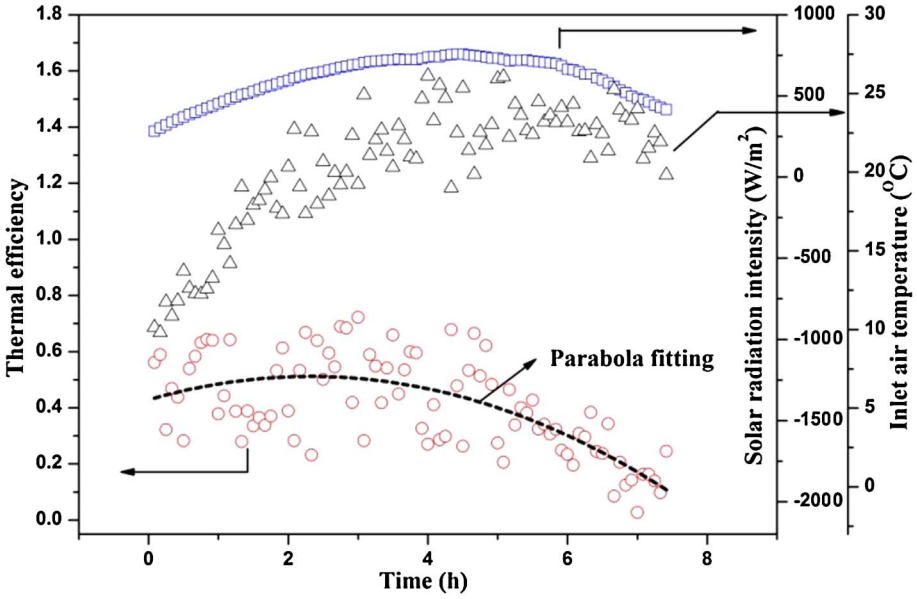

Fig. 6. Instantaneous thermal efficiencies for space heating in TC-Trombe wall.

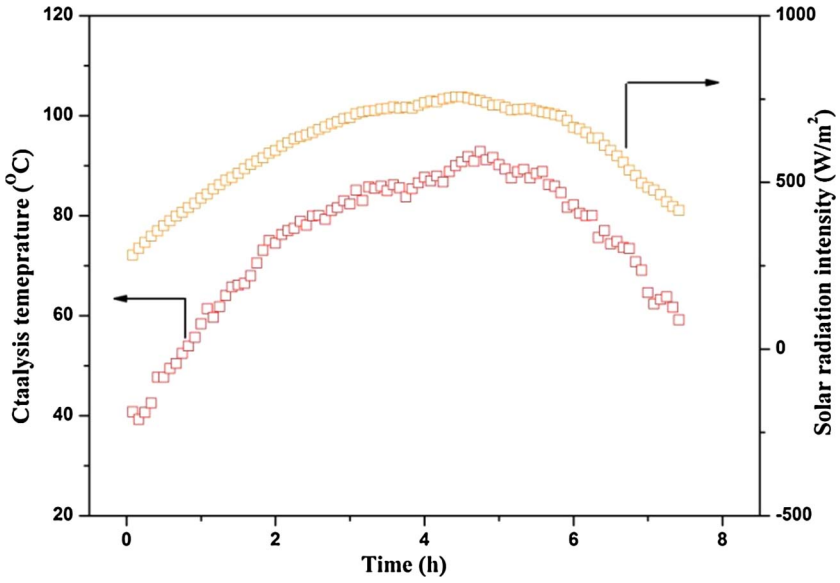

Fig. 7. Catalysts layer temperature in TC-Trombe wall.

pass conversion over MnO_x-CeO_2 under the solar radiation and in the dark under ambient temperature such as 25 °C (Fig. 11). Results showed that the formaldehyde single-pass conversion under PCO conditions was nearly the same as that of under TCO conditions. Therefore, the photocatalytic oxidation mechanism occupied little in TC-Trombe wall.

Apparently, the solar light driven TCO mechanism played a dominant role in TC-Trombe wall under full solar spectrum as schematically illustrated in Fig. 1. The photothermal conversion performance in full solar spectrum leaded a considerable temperature increase of MnO_x-CeO_2 catalysts layer (Figs. 4 and 7). The TCO reaction started when the temperature of MnO_x-CeO_2 catalysts approached to the start-off temperature. Mars-van Krevelen mechanism has been widely accepted to explain the TCO processes on metal oxides such as MnO_2, CeO_2, Co_3O_4 and their complexes [46,47,61,62,64–66]. Formaldehyde molecule adsorbed on the surface of MnO_x-CeO_2 catalysts is oxidized by the lattice oxygen of MnO_x-CeO_2. Then gas phase oxygen O_2 replenishes the reduced oxides by the reduction reaction. Therefore, the lattice oxygen activity plays a decisive role in the thermocatalytic reaction processes.

Fig. 11 further illustrated the effect of the solar radiation on the lattice oxygen activity in the TCO processes over catalysts MnO_x-CeO_2. A novel photoactivation effect existed in the solar light driven TCO mechanism. Similar photoactivation effect has been found for other catalysts such as Co_3O_4 [62] and MnO_2 [58]. The lattice oxygen of MnO_x-CeO_2 became more active under solar radiation. The enhancement of lattice oxygen activity accelerated the TCO processes. Therefore, a novel hybrid catalytic mechanism including the photothermal conversion, the solar light driven TCO mechanism and the photoactivation effect makes TC-Trombe wall system have the excellent catalytic activity for formaldehyde degradation under solar radiation.

5.3. Validation of the system thermal model

The air flow velocity is an important parameter to the established TC-Trombe wall model. The air flow is driven by the buoyancy lift, and the air flow velocity in the air cavity can be calculated through the pressure balance. The expression is as follows [15]:

$$V_a = \sqrt{\frac{g\beta(T_{out}-T_{in})H}{f_{in}(A/A_{in})^2 + f_{out}(A/A_{out})^2 + f(H/d)}} \quad (22)$$

where d is the hydrodynamic diameter of air cavity, m. A, A_{in} and A_{out}

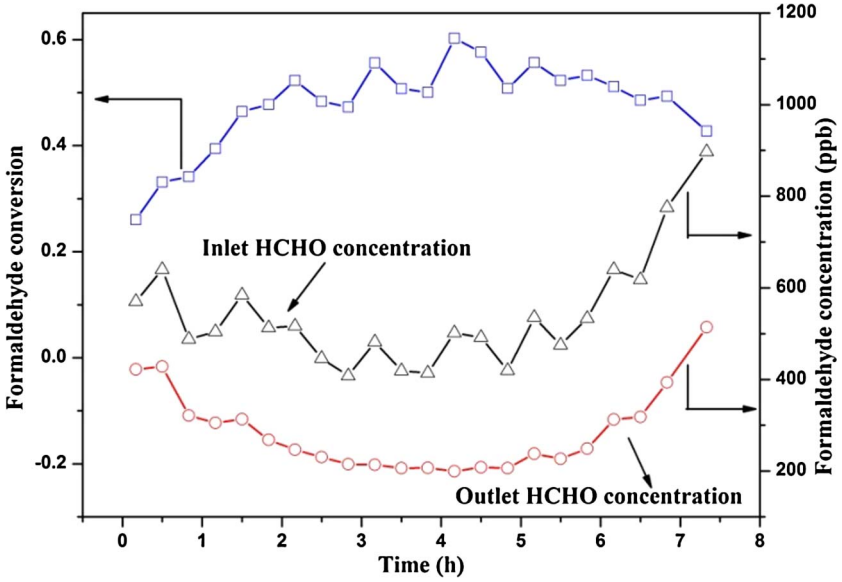

Fig. 8. Formaldehyde initial and outlet concentration and formaldehyde once-through conversion versus time in TC-Trombe wall.

are the cross area of air cavity, air inlet and air outlet, m^2, respectively. H is the height of air cavity, m. And f_{in} and f_{out} are the local resistance factor of the air inlet and outlet, respectively. Here $f_{in} = 1.0, f_{out} = 1.5$. f is the friction loss factors of air channel given by Blasius correlation for turbulent flow and the expression is as follows:

$$f = 0.3164Re^{-0.25} \tag{23}$$

Fig. 12 shows the comparison of the experimental and predicted air flow velocity calculated by equation (22) in the air cavity in TC-Trombe wall. The predicted data were in well agreement with the experimental data. The root mean square deviation (RSMD) value between the experimental and predicted data was 5.8%. And the error could be acceptable from the viewpoint of simplification. Therefore, the future calculations of air flow velocity were based on Eq. (22).

To validate the established system thermal model, the comparison of the measured and computational results of air outlet temperature and catalysts layer temperature was made. Figs. 13 and 14 depict experimental and computational results of air outlet temperature and catalysts layer temperature, respectively. Results showed that the resulting correspondence between the simulation and experimental data was good in most of the time. The RSMD values of air outlet temperature

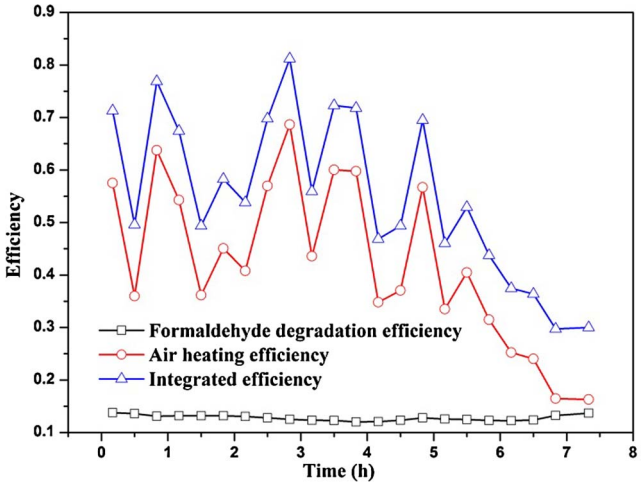

Fig. 10. The system efficiency curves of TC-Trombe wall including the thermal efficiency, formaldehyde removal efficiency and system integrated efficiency.

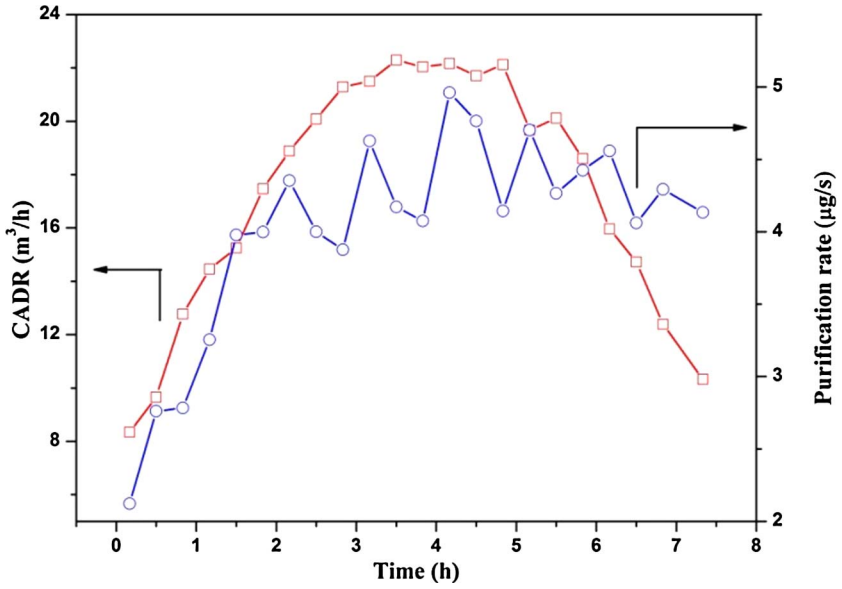

Fig. 9. The clean air delivery rate and purification rate versus time in TC-Trombe wall.

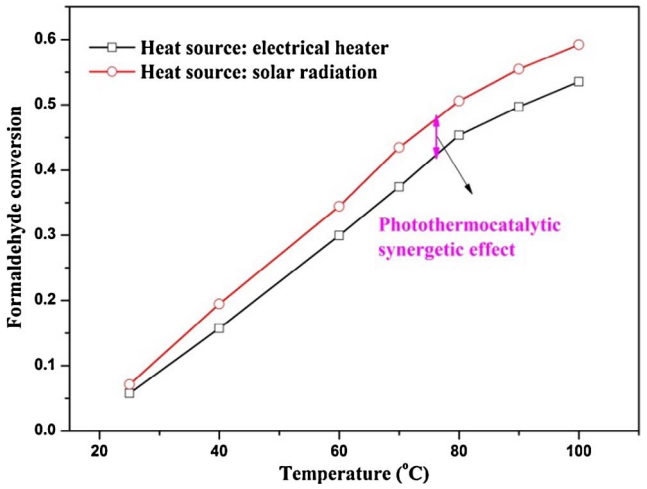

Fig. 11. The catalytic activity of MnO_x-CeO_2 for formaldehyde degradation at different temperature obtained by solar radiation or electrical heater at an initial concentration of 600 ppb.

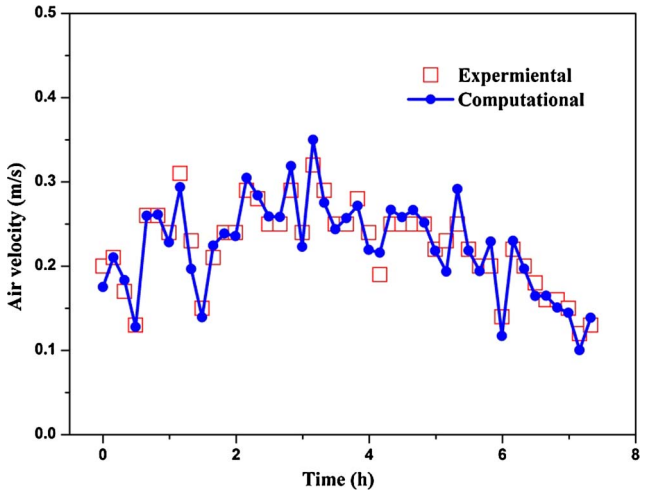

Fig. 12. Experimental and computational results of air flow velocity in the air cavity in TC-Trombe wall.

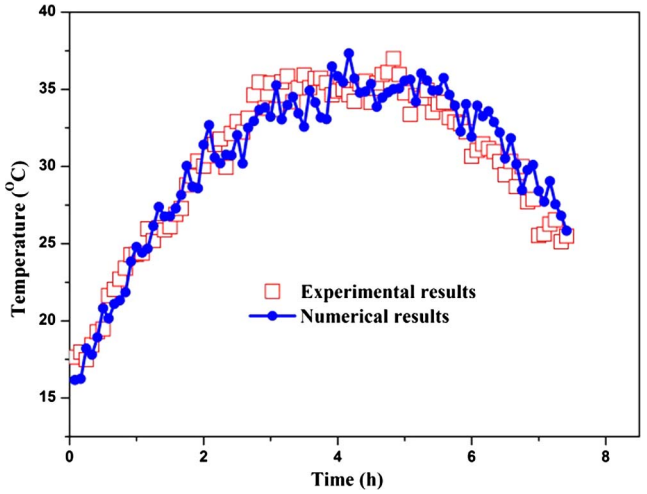

Fig. 13. Comparison of experimental and numerical temperature of air outlet temperature.

and catalysts layer temperature were 5.2% and 6.3%, respectively. The presence of errors was unavoidable due to the simplification of

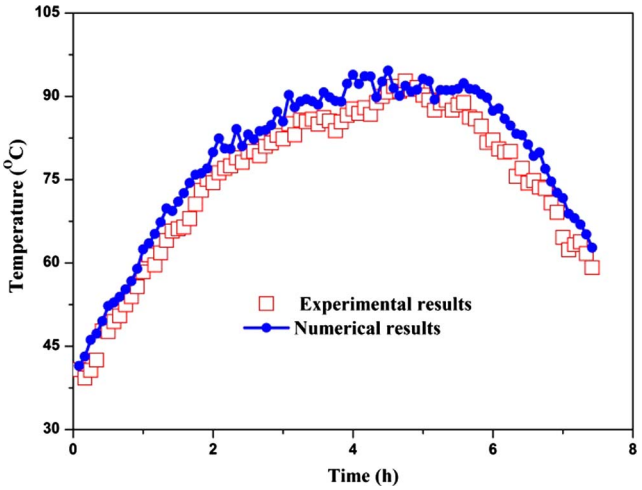

Fig. 14. Comparison of experimental and numerical temperature of catalysts layer temperature.

established thermal model. However, the RSMD values were acceptable in engineering. Therefore, the thermal properties of TC-Trombe wall were evaluated by the established thermal model.

5.4. Parametric study

Calculated by the proposed system thermal model, we studied the effects of meteorological parameters and structure parameters on the system efficiencies including the thermal efficiency, formaldehyde removal efficiency and system integrated efficiency.

Figs. 15 and 16 show the influences of meteorological parameters including solar radiation intensity and ambient temperature on the three efficiencies, respectively. In Fig. 15, the air heating efficiency increases as the increase of solar radiation intensity. As we known, as the increase of solar radiation intensity, the air temperature and air mass flow both increase and the increasing rate of air heat gain is bigger than that of solar radiation intensity. Therefore, according to the equation (1), the air heating efficiency presents an increasing trend as the solar radiation. However, formaldehyde degradation efficiency behaves an opposite tendency, which is the result of the increasing of heat loss caused by the temperature rise of catalysts layer. From Fig. 16, the ambient temperature has little effect on the three efficiencies.

Figs. 17 and 18 show the effects of structure parameters involving

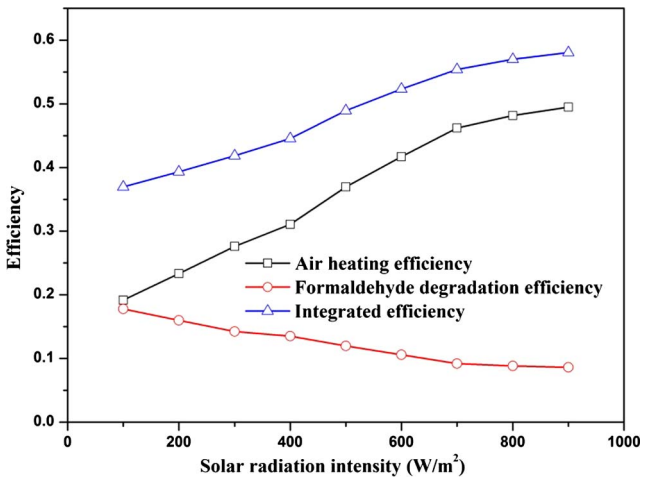

Fig. 15. The effect of solar radiation intensity on system efficiencies of TC-Trombe wall including the thermal efficiency, formaldehyde removal efficiency and system integrated efficiency. Ambient temperature: 10 °C.

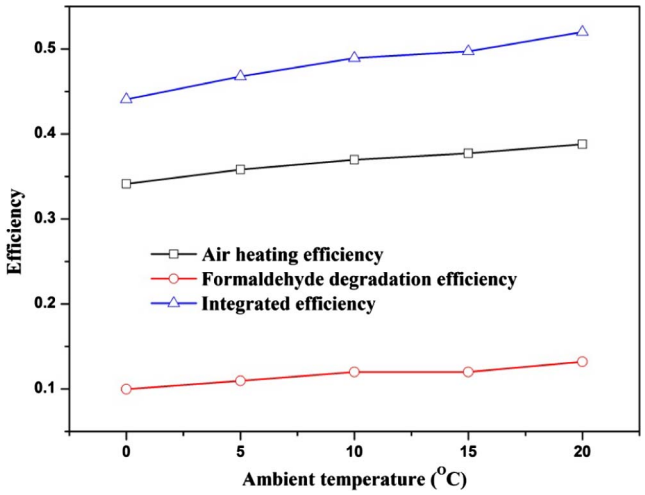

Fig. 16. The effect of ambient temperature on system efficiencies of TC-Trombe wall including the thermal efficiency, formaldehyde removal efficiency and system integrated efficiency. Solar radiation intensity: 500 W/m^2.

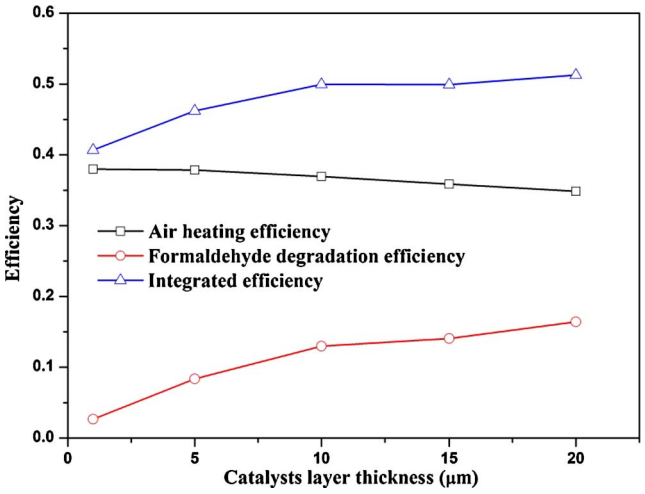

Fig. 17. The effect of catalysts layer thickness on system efficiencies of TC-Trombe wall including the thermal efficiency, formaldehyde removal efficiency and system integrated efficiency. Ambient temperature: 10 °C; Solar radiation intensity: 500 W/m^2.

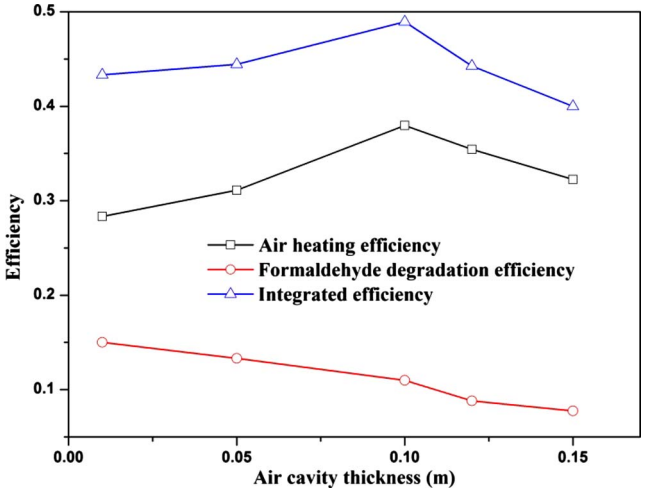

Fig. 18. The effect of air cavity thickness on system efficiencies of TC-Trombe wall including the thermal efficiency, formaldehyde removal efficiency and system integrated efficiency. Ambient temperature: 10 °C; Solar radiation intensity: 500 W/m^2.

the catalysts layer thickness and air cavity thickness on the three efficiencies, respectively. As the increase of the catalysts layer thickness, the absorbed heat by the catalysts layer increases because the used catalyst mass increases. However, the catalysts layer temperature varies small as the increase of the catalysts layer thickness through the calculations. Therefore, the formaldehyde degradation efficiency increases with the catalysts layer thickness. However, there is nearly no effect of the catalysts layer thickness on the air heating efficiency because the catalysts layer temperature nearly has no change. As shown in Fig. 18, the air cavity thickness has an optimal value. When the air cavity thickness is very thin, the air flow resistance becomes larger. The air mass flow decreases a lot. The main mode of heat transfer in the air cavity is thermal conduction not the conventional free convection and the heat-transfer capability decreases a lot. When the air cavity thickness is bigger, the air mass flow increases a lot and air temperature variation decreases. So the air heating efficiency exists a maximum when the air cavity thickness is 0.1 m. The formaldehyde degradation efficiency decreases because more heat is transferred to air with the rise of air layer thickness.

In summary, the excellent performance of TC-Trombe wall is determined by two factors. Firstly, the catalysts layer should have the strong absorption in whole region of solar spectrum and excellent photothermal conversion, which results in the considerable increase of catalyst temperature that is a crucial factor to the space heating and thermocatalytic reaction. The optimizing analysis of structure parameters based on the system model should be conducted to improve system heat collecting performance. Secondly, the catalyst should behave good thermocatalytic activity at low temperature.

5.5. Energy saving evaluation in heating seasons

The energy saving of TC-Trombe wall in heating seasons was analyzed in Hefei. The weather data of Hefei were provided by EnergyPlus. Fig. 19 shows the basic meteorological parameters including average hourly global solar radiation and ambient temperature in heating seasons. We assumed that TC-Trombe wall worked from 9:00 AM to 17:00 PM.

Fig. 20 presents the hourly variation of energy saving per unit TC-Trombe wall area in heating seasons. From the column diagram, the maximum saving energy can be obtained at 13:00 whether for air heating or for formaldehyde degradation. The variation trend is basically similar as that of global solar radiation. Fig. 21 shows the saving energy per unit TC-Trombe wall area under every month in heating seasons. As shown in Table 4, the monthly saving energy in every month are 32.5, 30.0 and 35 kW h/m^2 for TC-Trombe wall in heating seasons. The saving energy for formaldehyde degradation is 33.1 kW h/m^2. This part of saving energy is the thermal storage of the catalysts layer in the Trombe wall essentially. For conventional Trombe wall, this part of energy is only used for heating the air. In TC-Trombe wall system, at the time of heating the air for this part of energy, the high value-added clean air is obtained. And this part thermal energy is still used for space heating finally. The total saving energy is 97.4 kW h/m^2 in TC-Trombe wall system in Hefei.

6. Conclusions

A novel zero-energy solar application system combining the thermal catalytic oxidation technology with Trombe wall (TC-Trombe wall) without auxiliary energy was proposed. TC-Trombe wall has excellent indoor air purification performance fully driven by solar energy at the same time of heating air.

The full-day experiment results showed that TC-Trombe wall had the excellent space heating performance and formaldehyde degradation performance under solar radiation. Under the total solar radiation energy of 7.89 MJ, the daily air heating efficiency, generated total volume of fresh air and total formaldehyde degradation amount were 41.3%,

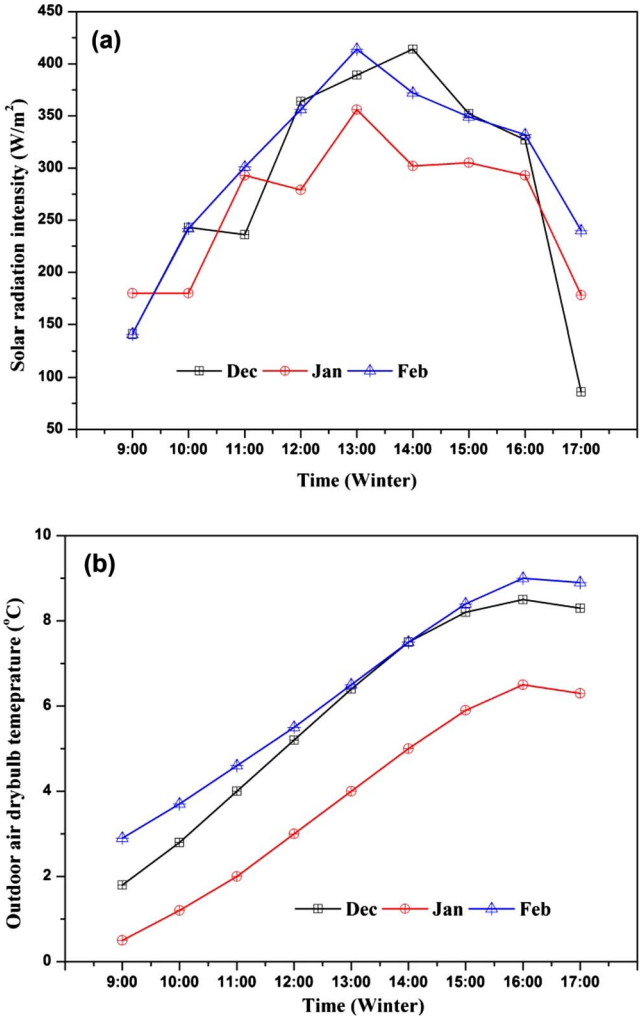

Fig. 19. Average hourly global solar radiation and outdoor air drybulb temperature in heating seasons in Hefei.

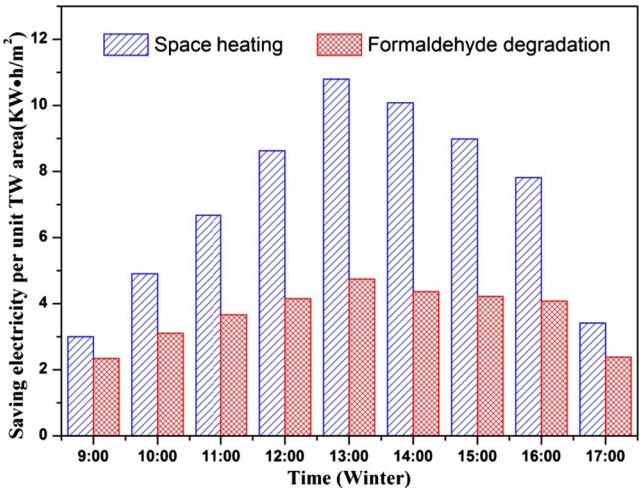

Fig. 20. Hourly variation of saving electricity per unit TC-Trombe wall area in heating seasons in Hefei.

249.2 $m^3/(m^2$ day) and 208.4 mg/(m^2 day), respectively. Significantly, a novel photoactivation effect exists in the solar light driven thermocatalytic oxidation processes. The lattice oxygen of the catalyst MnO_x-CeO_2 is activated under solar radiation and accelerates the thermocatalytic reaction. At the temperatures of 40, 60, 80 and 100 °C, the

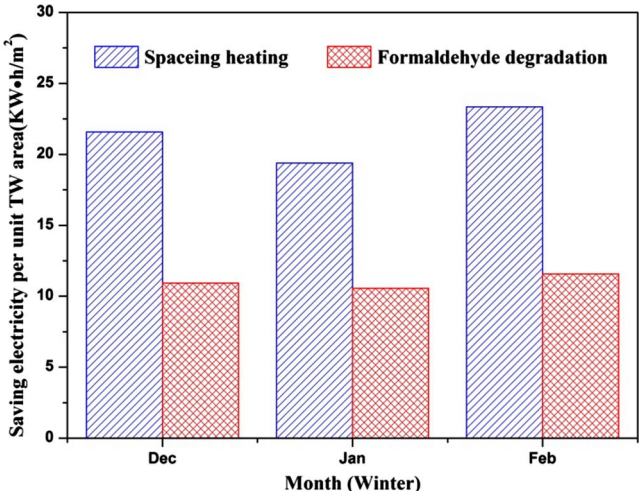

Fig. 21. The saving electricity per unit TC-Trombe wall area under different month in heating seasons in Hefei.

Table 4
The saving energy of TC-Trombe wall in heating seasons in Hefei.

	December	January	February
The monthly saving electricity (kW h/m^2)	32.5	30.0	35.0
The total monthly saving electricity (kW h/m^2)	97.4		

formaldehyde single-pass conversion under solar radiation were 1.3, 1.2, 1.2 and 1.1 times higher than that of in the dark, respectively. The photothermocatalytic synergetic effect indicates that TC-Trombe wall has huge potential for solar indoor air purification.

In addition, the proposed dynamic numerical model can well predict the experimental results. Model calculation results indicate the solar radiation intensity plays an import role for the system thermal performance while the effect of ambient temperature can be ignored. The air layer thickness exists an optimal value of 0.1 m to obtain the optimal integrated efficiency of TC-Trombe wall. Based on the established system thermal model, the energy saving performance of TC-Trombe wall was evaluated in heating seasons in Hefei. The saving energy for space heating and formaldehyde degradation are 64.3 kW h/m^2 and 33.1 kW h/m^2, respectively. And the saving energy consumption for formaldehyde degradation is the net benefits compared with conventional Trombe wall.

This paper presents the study of air heating performance and HCHO degradation performance of TC-Trombe wall based on the single-pass experimental results. For future studies on TC-Trombe wall system, the investigation on the system performance in the real rooms is needed. For the rear applications, the TC-Trombe wall, as one of improved Trombe wall technologies, is a very promising design that can obtained high thermal performance without auxiliary energy in buildings. And more importantly, this system can produce invaluable clean air, which is the one of the most precious products for human beings. TC-Trombe wall provides an energy-saving strategy for space heating and environmental cleanup using renewable solar energy and it has huge potential for the application of renewable solar energy on buildings.

Acknowledgments

This research was supported by the grants from Science and Technology Research project of Anhui Province (No. 1604e0302002), Beijing Advanced Innovation Center for Future Urban design (No. UDC2016040200), and also Program for Dongguan Innovative Research Team Program (No. 2014607101008).

References

[1] Díaz JJV, Wilby MR, González ABR. Setting up GHG-based energy efficiency targets in buildings: the Ecolabel. Energy Policy 2013;59:633–42.
[2] Zhang T, Tan Y, Yang H, Zhang X. The application of air layers in building envelopes: a review. Appl Energy 2016;165:707–34.
[3] Omrany H, Ghaffarianhoseini A, Ghaffarianhoseini A, Raahemifar K, Tookey J. Application of passive wall systems for improving the energy efficiency in buildings: a comprehensive review. Renew Sustain Energy Rev 2016;62:1252–69.
[4] Llovera J, Potau X, Medrano M, Cabeza LF. Design and performance of energy-efficient solar residential house in Andorra. Appl Energy 2011;88:1343–53.
[5] Abbassi F, Dimassi N, Dehmani L. Energetic study of a Trombe wall system under different Tunisian building configurations. Energy Build 2014;80:302–8.
[6] Hassanain A, Hokam E, Mallick T. Effect of solar storage wall on the passive solar heating constructions. Energy Build 2011;43:737–47.
[7] Hernández-López I, Xamán J, Chávez Y, Hernández-Pérez I, Alvarado-Juárez R. Thermal energy storage and losses in a room-Trombe wall system located in Mexico. Energy 2016;109:512–24.
[8] Liu Y, Wang D, Ma C, Liu J. A numerical and experimental analysis of the air vent management and heat storage characteristics of a trombe wall. Sol Energy 2013;91:1–10.
[9] Rabani M, Kalantar V, Faghih AK, Rabani M, Rabani R. Numerical simulation of a Trombe wall to predict the energy storage rate and time duration of room heating during the non-sunny periods. Heat Mass Transfer 2013;49:1395–404.
[10] Bojić M, Johannes K, Kuznik F. Optimizing energy and environmental performance of passive Trombe wall. Energy Build 2014;70:279–86.
[11] Briga-Sá A, Martins A, Boaventura-Cunha J, Lanzinha JC, Paiva A. Energy performance of Trombe walls: adaptation of ISO 13790: 2008 (E) to the Portuguese reality. Energy Build 2014;74:111–9.
[12] Zhou G, Pang M. Experimental investigations on the performance of a collector–-storage wall system using phase change materials. Energy Convers Manage 2015;105:178–88.
[13] Rabani M, Kalantar V, Dehghan AA, Faghih AK. Experimental study of the heating performance of a Trombe wall with a new design. Sol Energy 2015;118:359–74.
[14] Shen J, Lassue S, Zalewski L, Huang D. Numerical study of classical and composite solar walls by TRNSYS. J Therm Sci 2007;16:46–55.
[15] Sun W, Ji J, Luo C, He W. Performance of PV-Trombe wall in winter correlated with south façade design. Appl Energy 2011;88:224–31.
[16] Shen J, Lassue S, Zalewski L, Huang D. Numerical study on thermal behavior of classical or composite Trombe solar walls. Energy Build 2007;39:962–74.
[17] Saadatian O, Sopian K, Lim CH, Asim N, Sulaiman MY. Trombe walls: a review of opportunities and challenges in research and development. Renew Sustain Energy Rev 2012;16:6340–51.
[18] Tunç M, Uysal M. Passive solar heating of buildings using a fluidized bed plus Trombe wall system. Appl Energy 1991;38:199–213.
[19] Chen W, Liu W. Numerical analysis of heat transfer in a composite wall solar-collector system with a porous absorber. Appl Energy 2004;78:137–49.
[20] Agrawal B, Tiwari G. Optimizing the energy and exergy of building integrated photovoltaic thermal (BIPVT) systems under cold climatic conditions. Appl Energy 2010;87:417–26.
[21] Luo Y, Zhang L, Liu Z, Wang Y, Meng F, Wu J. Thermal performance evaluation of an active building integrated photovoltaic thermoelectric wall system. Appl Energy 2016;177:25–39.
[22] Chow TT. A review on photovoltaic/thermal hybrid solar technology. Appl Energy 2010;87:365–79.
[23] Jiang B, Ji J, Yi H. The influence of PV coverage ratio on thermal and electrical performance of photovoltaic-Trombe wall. Renew Energy 2008;33:2491–8.
[24] Jie J, Hua Y, Wei H, Gang P, Jianping L, Bin J. Modeling of a novel Trombe wall with PV cells. Build Environ 2007;42:1544–52.
[25] Jie J, Hua Y, Gang P, Bin J, Wei H. Study of PV-Trombe wall assisted with DC fan. Build Environ 2007;42:3529–39.
[26] Buonomano A, Calise F, Palombo A, Vicidomini M. BIPVT systems for residential applications: an energy and economic analysis for European climates. Appl Energy 2016;184:1411–31.
[27] Zogou O, Stapountzis H. Energy analysis of an improved concept of integrated PV panels in an office building in central Greece. Appl Energy 2011;88:853–66.
[28] Slimani MEA, Amirat M, Kurucz I, Bahria S, Hamidat A, Chaouch WB. A detailed thermal-electrical model of three photovoltaic/thermal (PV/T) hybrid air collectors and photovoltaic (PV) module: Comparative study under Algiers climatic conditions. Energy Convers Manage 2017;133:458–76.
[29] Dehra H. An investigation on energy performance assessment of a photovoltaic solar wall under buoyancy-induced and fan-assisted ventilation system. Appl Energy 2017;191:55–74.
[30] Vats K, Tiwari G. Energy and exergy analysis of a building integrated semi-transparent photovoltaic thermal (BISPVT) system. Appl Energy 2012;96:409–16.
[31] Luo Y, Zhang L, Wang X, Xie L, Liu Z, Wu J, et al. A comparative study on thermal performance evaluation of a new double skin façade system integrated with photovoltaic blinds. Appl Energy 2017;199:281–93.
[32] Luo Y, Zhang L, Wu J, Liu Z, Wu Z, He X. Dynamical simulation of building integrated photovoltaic thermoelectric wall system: Balancing calculation speed and accuracy. Appl Energy 2017.
[33] Tham KW. Indoor air quality and its effects on humans—a review of challenges and developments in the last 30 years. Energy Build 2016;130:637–50.
[34] Zhang Y, Mo J, Li Y, Sundell J, Wargocki P, Zhang J, et al. Can commonly-used fan-driven air cleaning technologies improve indoor air quality? A literature review. Atmos Environ 2011;45:4329–43.
[35] Cao G, Awbi H, Yao R, Fan Y, Sirén K, Kosonen R, et al. A review of the performance of different ventilation and airflow distribution systems in buildings. Build Environ 2014;73:171–86.
[36] Tong Z, Chen Y, Malkawi A, Liu Z, Freeman RB. Energy saving potential of natural ventilation in China: The impact of ambient air pollution. Appl Energy 2016;179:660–8.
[37] Ben-David T, Waring MS. Impact of natural versus mechanical ventilation on simulated indoor air quality and energy consumption in offices in fourteen US cities. Build Environ 2016;104:320–36.
[38] Martins NR, da Graça GC. Impact of outdoor PM2. 5 on natural ventilation usability in California's nondomestic buildings. Appl Energy 2017;189:711–24.
[39] Oropeza-Perez I, Østergaard PA. Potential of natural ventilation in temperate countries–a case study of Denmark. Appl Energy 2014;114:520–30.
[40] Cui X, Mohan B, Islam M, Chou S, Chua K. Energy performance evaluation and application of an air treatment system for conditioning building spaces in tropics. Appl Energy 2017.
[41] Huang H, Xu Y, Feng Q, Leung DY. Low temperature catalytic oxidation of volatile organic compounds: a review. Catal Sci Technol 2015;5:2649–69.
[42] Zhong L, Haghighat F. Photocatalytic air cleaners and materials technologies–-abilities and limitations. Build Environ 2015;91:191–203.
[43] Yu B, He W, Li N, Yang F, Ji J. Thermal catalytic oxidation performance study of SWTCO system for the degradation of indoor formaldehyde: kinetics and feasibility analysis. Build Environ 2016;108:183–93.
[44] Pei J, Han X, Lu Y. Performance and kinetics of catalytic oxidation of formaldehyde over copper manganese oxide catalyst. Build Environ 2015;84:134–41.
[45] Xu Q, Zhang Y, Mo J, Li X. Indoor formaldehyde removal by thermal catalyst: kinetic characteristics, key parameters, and temperature influence. Environ Sci Technol 2011;45:5754–60.
[46] Tang X, Chen J, Huang X, Xu Y, Shen W. Pt/MnO x–CeO2 catalysts for the complete oxidation of formaldehyde at ambient temperature. Appl Catal B-Environ 2008;81:115–21.
[47] Tang X, Li Y, Huang X, Xu Y, Zhu H, Wang J, et al. MnO x–CeO 2 mixed oxide catalysts for complete oxidation of formaldehyde: effect of preparation method and calcination temperature. Appl Catal B-Environ 2006;62:265–73.
[48] Salthammer T, Mentese S, Marutzky R. Formaldehyde in the indoor environment. Chem Rev 2010;110:2536–72.
[49] Foarde KK. Methodology to perform clean air delivery rate type determinations with microbiological aerosols. Aerosol Sci Tech 1999;30:235–45.
[50] Shaughnessy RJ, Levetin E, Blocker J, Sublette KL. Effectiveness of portable indoor air cleaners: sensory testing results. Indoor Air 1994;4:179–88.
[51] Bergman TL, Incropera FP, DeWitt DP, Lavine AS. Fundamentals of heat and mass transfer. John Wiley & Sons; 2011.
[52] Duan S, Jing C, Zhao Z. Energy and exergy analysis of different Trombe walls. Energy Build 2016;126:517–23.
[53] Bellos E, Tzivanidis C, Zisopoulou E, Mitsopoulos G, Antonopoulos KA. An innovative Trombe wall as a passive heating system for a building in Athens—a comparison with the conventional Trombe wall and the insulated wall. Energy Build 2016;133:754–69.
[54] Plaisance H, Blondel A, Desauziers V, Mocho P. Characteristics of formaldehyde emissions from indoor materials assessed by a method using passive flux sampler measurements. Build Environ 2014;73:249–55.
[55] Tang X, Bai Y, Duong A, Smith MT, Li L, Zhang L. Formaldehyde in China: production, consumption, exposure levels, and health effects. Environ Int 2009;35:1210–24.
[56] Chen W, Zhang JS, Zhang Z. Performance of air cleaners for removing multiple volatile organic compounds in indoor air. ASHRAE Trans 2005;111:1101–14.
[57] Yu B, He W, Li N, Zhou F, Shen Z, Chen H, et al. Experiments and kinetics of solar PCO for indoor air purification in PCO/TW system. Build Environ 2017;115:130–46.
[58] Liu F, Zeng M, Li Y, Yang Y, Mao M, Zhao X. UV–Vis–infrared light driven thermocatalytic activity of octahedral layered birnessite nanoflowers enhanced by a novel photoactivation. Adv Func Mater 2016;26:4518–26.
[59] Ching W, Leung M, Leung DY. Solar photocatalytic degradation of gaseous formaldehyde by sol–gel TiO2 thin film for enhancement of indoor air quality. Sol Energy 2004;77:129–35.
[60] Spasiano D, Marotta R, Malato S, Fernandez-Ibanez P, Di Somma I. Solar photocatalysis: materials, reactors, some commercial, and pre-industrialized applications. A comprehensive approach. Appl Catal B-Environ 2015;170:90–123.
[61] Mao M, Li Y, Hou J, Zeng M, Zhao X. Extremely efficient full solar spectrum light driven thermocatalytic activity for the oxidation of VOCs on OMS-2 nanorod catalyst. Appl Catal B-Environ 2015;174:496–503.
[62] Zheng Y, Wang W, Jiang D, Zhang L, Li X, Wang Z. Ultrathin mesoporous Co3O4 nanosheets with excellent photo-/thermo-catalytic activity. J Mater Chem A 2016;4:105–12.
[63] Hou J, Li Y, Mao M, Yue Y, Greaves GN, Zhao X. Full solar spectrum light driven thermocatalysis with extremely high efficiency on nanostructured Ce ion substituted OMS-2 catalyst for VOCs purification. Nanoscale 2015;7:2633–40.
[64] Tang X, Chen J, Li Y, Li Y, Xu Y, Shen W. Complete oxidation of formaldehyde over Ag/MnO x–CeO2 catalysts. Chem Eng J 2006;118:119–25.
[65] Zeng M, Li Y, Mao M, Bai J, Ren L, Zhao X. Synergetic effect between photocatalysis on TiO2 and thermocatalysis on CeO2 for gas-phase oxidation of benzene on TiO2/CeO2 nanocomposites. ACS Catal 2015;5:3278–86.
[66] Zheng Y, Wang W, Jiang D, Zhang L. Amorphous MnOx modified Co 3 O 4 for formaldehyde oxidation: improved low-temperature catalytic and photo-thermocatalytic activity. Chem Eng J 2016;284:21–7.